$a_s = 3.31 \times 10^{-8}$ cm (Ta); $a_s = 3.3 \times 10^{-8}$ cm (Nb).

Thus, the theoretical values of ε agree well with those obtained in experiment. The physical argument in favor of the assumption that the conduction electrons do not enter into the volume of the scatterer is the fact that otherwise ε would depend on the relaxation time in the scatterer volume and would decrease with decreasing temperature. In our case, both the size dependence and the temperature dependence of the total line width are well accounted for by temperature-independent values of ε.

One of the possible mechanisms of the scattering of the sodium conduction electrons by the interface may be resonant scattering by the d-orbitals of the first layer of the scatterer which form a band of surface states[10] at the surface of the free scatterer crystal, this band being located near the Fermi level. In the case of the contact of the scatterer layer with sodium, the surface-state band should broaden. The situation recalls resonant scattering by virtual d states of the impurity atom. Comparing the known expression for the effective cross section for resonant scattering, with spin flip, by an impurity located in the volume of the sodium, and the value of σ_s calculated from the experimentally obtained value of ε, we can estimate the broadening of the surface-state band: $\Gamma(\text{Na-Nb}) \approx \Gamma(\text{Na-Ta}) = 3$ eV. It should be noted that the question of the scattering mechanism calls for further theoretical and experimental research.

[1]I. G. Zamaleev and E. G. Kharakhash'yan, Pis'ma Zh. Eksp. Teor. Fiz. **27**, 677 (1978) [JETP Lett. **27**, 641 (1978)].
[2]F. J. Dyson, Phys. Rev. **98**, 349 (1955).
[3]M. B Walker, Phys. Rev. **B3**, 30 (1971).
[4]V. V. Ustinov, Fiz. Met. Metalloved. **45**, 473 (1978).
[5]V. N. Lisin, Zh. Eksp. Teor. Fiz. **72**, 573 (1977) [Sov. Phys. JETP **45**, 300 (1977)].
[6]J. H. Pifer and R. Magno, Phys. Rev. **B3**, 661 (1971).
[7]Spravochnik po fiziko-tekhnicheskim osnovam kriogeniki (Handbook of Physical and Technical Principles of Cryogenics), M. P. Malkov, ed., Energiya, 1973.
[8]D. Pines and F. Slichter, Phys. Rev. **100**, 1014 (1955).
[9]J. S. Griffith, The Theory of Transition Metal Ions, Cambridge Un. Press, 1961.
[10]St. G. Louie, Kai-Ming Ho, J. R. Chelikowsky, and M. L. Cohen, Phys. Rev. **B15**, 5627 (1977).

Translated by J. G. Adashko

Transport of polarized radiation in crystals in the excitonic region of the spectrum. Polariton effects

E. L. Ivchenko, G. E. Pikus, and N. Kh. Yuldashev

A. F. Ioffe Physicotechnical Institute, USSR Academy of Sciences

(Submitted 3 August 1980)
Zh. Eksp. Teor. Fiz. **80**, 1228–1245 (March 1981)

A theory is developed for radiation transport in crystals with allowance for polariton effects in elastic scattering of the polaritons by impurity centers. The frequency dependences of the intensity and of the degree of polarization of the resonant secondary emission upon excitation by polarized light are calculated and analyzed. It is shown that the analysis of polariton transport in the absence of spatial dispersion, when the exciton effective mass $M \to \infty$, reduces to the problem of radiation transport in a turbid medium. At a finite exciton effective mass, account was taken of the additional light waves. In the region below the longitudinal frequency ω_L, the presence of additional waves that attenutate in space at $\omega < \omega_L$ influences only the polariton reflection coefficients. In the frequency region above ω_L an important role is played by scattering processes between two transverse-wave branches and between branches of transverse and longitudinal polaritons.

PACS numbers: 79.60. – i, 71.36. + c, 71.35. + z

§1. INTRODUCTION

In our preceding paper[1] we developed a theory of resonant transport of polarized radiation in crystals, with account taken of the reabsorption and reemission as well as of multiple reflection of light from the surface. The analysis was carried out in the limiting case of weak exciton-photon interaction, when the photons and excitons could be regarded as separate particles. The present article is devoted to a study of transport of resonant radiation in crystals in the case of strong exciton-photon interaction, which leads to a restructuring of the energy spectrum of the photon and excitons, and to formation of collective modes–polaritons (opto-excitons).

Interest in the theory of polariton transport has increased in connection with the observation and investigation of resonant Brillouin scattering of polaritons in III–V semiconductors (GaAs) and II–VI semiconductors (CdS, CdSe).[2-5] In most theoretical work on resonant scattering of polaritons, only single scattering was taken into account.[6-8] In the general case, however, before a polariton is emitted into vacuum or recombines nonradiatively, it undergoes multiple scattering. The Brillouin spectrum revealed therefore not only single-phonon but also two-phonon peaks, as well as a broad background corresponding to multiple scattering (the so-called polariton fluorescence).[4] As shown by experiment,[9] the distribution function of the polaritons is inhomogeneous in space and has greatly differing values near the boundary and in the interior of the sample.

0038-5646/81/030629-10$02.40

In the present paper we develop a general method that makes it possible to take into account multiple scattering of the polaritons. Just as in Ref. 1, we consider dipole-active exciton resonance with isotropic effective mass in a crystal of cubic symmetry, and take into account only elastic scattering of polaritons by impurities. The method developed allows us to take into account the additional light waves (in the presence of spatial dispersion), the polarization of the polariton waves, the inhomogeneity of the distribution of the polaritons in space, and the reflection of the polaritons from the inner boundary of the crystal. The results obtained in the present paper explain the main features of multiple resonant scattering of light and uncover a possibility of task-oriented organization of experiments on the study of diffuse scattering of polaritons.

§2. GENERAL RELATIONS

For a dipole-active exciton with isotropic effective mass in a cubic crystal, the polariton spectrum in the vicinity of the resonant frequency ω_0 consists of two transverse-wave branches (branches 1 and 2 in Fig. 1), determined by the dispersion relation

$$\left(\frac{ck}{\omega}\right)^2=\varepsilon_0+\frac{\varepsilon_0\omega_{LT}}{\omega_0(k)-\omega} \tag{1}$$

and one longitudinal-exciton branch (branch 3 in Fig. 1)

$$\omega_3(k)=\omega_0(k)+\omega_{LT}, \tag{2}$$

where c is the speed of light in vacuum, $\mathbf{k}$ is the wave vector, ε_0 is the background dielectric constant, $\hbar\omega_0(k)=\hbar\omega_0+(\hbar^2k^2/2M)$ is the energy of the mechanical exciton in a state with wave vector $\mathbf{k}$, M is the effective mass of the exciton, $\omega_{LT}=\omega_3(0)-\omega_0$ is the longitudinal-transverse splitting. Here and elsewhere we assume that $\omega_{LT}\ll\omega_0$, and confine ourselves to the frequency region near ω_0:

$$|\omega-\omega_0|\ll\omega_0. \tag{3}$$

The intensity and the polarization state of the transverse polaritons propagating in the Ω direction will be described, as in the case of ordinary light [see Ref. 1, Eq. (2)] by the 4-vectors

$$\mathbf{I}^{(\beta)}=\begin{bmatrix} I_l^{(\beta)} \\ I_r^{(\beta)} \\ U^{(\beta)} \\ V^{(\beta)} \end{bmatrix} \quad (\beta=1,2). \tag{4}$$

The intensity $I^{(\beta)}=I_l^{(\beta)}+I_r^{(\beta)}$ is connected with the polariton distribution function $N_\beta(\Omega)$ by the relation

$$I^{(\beta)}(\Omega)=\hbar\omega v_\beta N_\beta(\Omega), \tag{5}$$

where $v_\beta=\partial\omega_\beta(k)/\partial k$ is the group velocity. For longitudinal excitons propagating in the Ω direction, the matrix $\mathbf{I}^{(3)}$ has one component, namely the intensity $I^{(3)}(\Omega)$. The longitudinal-exciton velocity is then $v_3=\hbar k/M$.

In analogy with Ref. 1, we assume that the crystal boundary is irradiated by a monochromatic light wave of frequency ω with total flux $\pi\mathbf{F}$ per unit area perpendicular to the propagation direction, and take into account only the elastic scattering of the polaritons by the impurity centers. Therefore the frequency of the radiation emerging from the crystal coincides with the frequency of the exciting light.

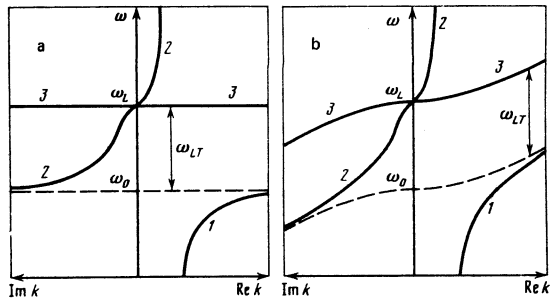

FIG. 1. Dispersion curves of polaritons in the absence (a) and in the presence (b) of spatial dispersion (dashed–dispersion curve of mechanical exciton).

A generalization of the radiation transport equation [see Ref. 1, Eq. (5)] is a system of equations for $\mathbf{I}^{(\beta)}(z,\Omega)$ $(\beta=1,2,3)$:

$$\mu\frac{\partial\mathbf{I}^{(\beta)}(z,\Omega)}{\partial z}=\alpha_\beta\mathbf{I}^{(\beta)}(z,\Omega)-\sum_{\beta'}\int\frac{d\Omega'}{4\pi}a_{\beta\beta'}\mathbf{P}_{\beta\beta'}(\Omega,\Omega')\mathbf{I}^{(\beta')}(z,\Omega')$$

$$-\frac{1}{4}\sum_{\beta'}a_{\beta\beta'}\mathbf{P}_{\beta\beta'}(\Omega,\Omega_{0\beta'})\mathbf{F}^{(\beta')}\exp\left(-\frac{\alpha_{\beta'}z}{|\mu_{0\beta'}|}\right), \tag{6}$$

where z is the coordinate in the direction of the inward normal to the crystal surface, $\mu=\cos\theta$, θ is the angle between Ω and the $(-z)$ axis, and α_β is the absorption coefficient of the β wave. We have separated in (6) the term connected with the contribution of the (attenuated) primary fluxes $\pi\mathbf{F}^{(\beta)}$ that travel in the crystal in the $\Omega_{0\beta}$ directions. Therefore the quantities $\mathbf{I}^{(\beta)}(z,\Omega)$ in (6) characterize the diffuse-radiation field. The total scattering matrix of the polariton from branch β' into β is written in (6) in the form of the product of the scalar coefficient $a_{\beta\beta'}$ and the scattering matrix $\mathbf{P}_{\beta\beta'}(\Omega,\Omega')$, which has a dimensionality $h_\beta^2\times h_{\beta'}^2$, where h_β is the degeneracy multiplicity of the polariton branch $\beta(h_{1,2}=2,\ h_3=1)$. We shall find it next to normalize $\mathbf{P}_{\beta\beta'}(\Omega,\Omega')$ in such a way that

$$\sum_{i=1}^{h_\beta}\int\frac{d\Omega}{4\pi}P_{\beta\beta',ii'}(\Omega,\Omega')=\frac{h_\beta}{2}. \tag{7}$$

At $\beta,\beta'=1,2$ the normalization (7) coincides with the normalization of the matrix $\mathbf{P}(\Omega,\Omega)$ in Ref. 1, [Eq. (6)].

We consider hereafter the case of a short-range scattering potential $V(\mathbf{r})$, when the q-dependence of the Fourier component $V(\mathbf{q})=\int d\mathbf{r}\exp(-i\mathbf{q}\cdot\mathbf{r})V(\mathbf{r})$ can be neglected, and $V(\mathbf{q})=V_0$ can be assumed. In this case the probability of scattering of the polariton with polarization $\mathbf{e}'$ into a state with polarization $\mathbf{e}$ is proportional to $|\mathbf{e}^*\cdot\mathbf{e}'|^2$. To determine the matrix $\mathbf{P}_{\beta\beta'}(\Omega,\Omega')$ we change from the basis (4) to the basis $d_{ij}^{(\beta)}\sim\langle E_i^{(\beta)}E_j^{(\beta)*}\rangle$. We use here for the transverse branches 1 and 2 the indices $i,j=l,r$, where the l axis lies in the plane containing the vector Ω and the z axis, while the r axis is perpendicular to this plane; for the longitudinal branch 3 we have $i=j=\Omega$. The transition from the d-basis to the basis (4) is with the aid of the matrices

$$U_{1,2}=\begin{bmatrix}1&0&0&0\\0&1&0&0\\0&0&1&1\\0&0&-i&i\end{bmatrix},\quad U_3=1. \tag{8}$$

In scattering by a short-range potential we have in the d-basis

$$P_{\beta\beta';ij,i'j'}(\Omega,\Omega')=\tfrac{3}{2}(e_i^{(\beta)*}(\Omega)e_{i'}^{(\beta')}(\Omega'))(e_j^{(\beta)}(\Omega)e_{j'}^{(\beta')*}(\Omega'))$$
$$=\tfrac{3}{2}\sum_{\eta,\xi=x,y,z}e_{i\eta}^{(\beta)*}(\Omega)e_{j\xi}^{(\beta)}(\Omega)e_{i'\eta}^{(\beta')}(\Omega')e_{j'\xi}^{(\beta')*}(\Omega'), \tag{9}$$

where $\mathbf{e}_i^{(\beta)}$ is a unit vector in the direction of the axis l or r at $\beta=1$, 2 and in the direction Ω at $\beta=3$. The factor $3/2$ in (9) ensures satisfaction of the normalization (7). We introduce the matrices $\Theta_\beta(\Omega)$ with components

$$\Theta_{\beta;ij,\eta\xi}(\Omega)=e_{i\eta}^{(\beta)*}(\Omega)e_{j\xi}^{(\beta)}(\Omega). \tag{10}$$

These matrices have dimensionality $h_\beta^2\times 9$. Then the expression for the scattering matrix $\mathbf{P}_{\beta\beta'}(\Omega,\Omega')$ in the basis (4) can be written in factorized form

$$\mathbf{P}_{\beta\beta'}(\Omega,\Omega')=\tfrac{3}{2}\mathbf{U}_\beta\Theta_\beta(\Omega)\Theta_{\beta'}^{+}(\Omega')\mathbf{U}_{\beta'}^{-1}. \tag{11}$$

The matrices $\mathbf{P}_{\beta\beta'}(\Omega,\Omega')$ admit of an expansion similar to Eq. (6) of Ref. 1:

$$\mathbf{P}_{\beta\beta'}(\Omega,\Omega')=\tfrac{3}{4}\mathbf{P}_{\beta\beta'}^{(0)}(\mu,\mu')+[(1-\mu^2)(1-\mu'^2)]^{1/4}$$
$$\times\mathbf{P}_{\beta\beta'}^{(1)}(\Omega,\Omega')+\mathbf{P}_{\beta\beta'}^{(2)}(\Omega,\Omega'), \tag{12}$$

and the components of the matrices $\mathbf{P}_{\beta\beta'}^{(m)}(\Omega,\Omega)$ contain $\cos m\psi$ or $\sin m\psi$ ($\psi=\varphi'-\varphi$). We note that we have not separated in (12) the matrix $\mathbf{Q}$ as an explicit factor [see Eq. (6) of Ref. 1]. For $\beta,\beta'=1$, 2 we therefore have

$$\mathbf{P}_{\beta\beta'}^{(m)}(\Omega,\Omega')=\mathbf{Q}\mathbf{P}^{(m)}(\Omega,\Omega'),$$

where $\mathbf{P}^{(m)}$ are the matrices introduced in Eq. (6) of Ref. 1.

The matrices $\mathbf{P}_{\beta\beta'}^{(0)}(\mu,\mu')$, which do not depend on the azimuthal angles, can also be represented in factorized form

$$\mathbf{P}_{\beta\beta'}^{(0)}(\mu,\mu')=\mathbf{M}_\beta(\mu)\tilde{\mathbf{M}}_{\beta'}(\mu'), \tag{13}$$

where

$$\mathbf{M}_{1,2}(\mu)=\begin{bmatrix}\mu^2&2^{1/2}(1-\mu^2)&0\\1&0&0\\0&0&0\\0&0&2^{1/2}\mu\end{bmatrix},\quad \mathbf{M}_3(\mu)=(1-\mu^2,\,2^{1/2}\mu^2,\,0).$$

To obtain the representation (13), it suffices to average $\Theta_\beta(\Omega)$ in (11) over the azimuthal angle φ, bearing it in mind that

$$\mathbf{P}_{\beta\beta'}^{(0)}(\mu,\mu')=\tfrac{1}{2}\overline{\mathbf{P}_{\beta\beta'}(\Omega,\Omega')}_\varphi=2\mathbf{U}_\beta\overline{\Theta_\beta(\Omega)}_\varphi\overline{\Theta_{\beta'}^{+}(\Omega')}_\varphi\mathbf{U}_{\beta'}^{-1},$$

and recognizing that a number of columns of the matrix $[\Theta(\Omega)]_\varphi$ consist of zeros, and that many nonzero components of this matrix are linearly dependent.

We present also expressions for the matrices

$$\mathbf{P}_{\beta3}^{(m)}(\Omega,\Omega')=\tilde{\mathbf{P}}_{3\beta}^{(m)}(\Omega',\Omega)\mathbf{Q}^{-1}\ \text{и}\ P_{33}^{(m)}(\Omega,\Omega')\quad(m=1,2;\ \beta=1,2):$$

$$\mathbf{P}_{\beta3}^{(1)}(\Omega,\Omega')=\frac{3}{2}\begin{bmatrix}-2\mu\mu'\cos\psi\\0\\\mu'\sin\psi\\0\end{bmatrix},\quad \mathbf{P}_{\beta3}^{(2)}(\Omega,\Omega')=\frac{3}{4}(1-\mu'^2)\begin{bmatrix}\mu^2\cos2\psi\\-\cos2\psi\\-2\sin2\psi\\0\end{bmatrix}, \tag{14}$$

$$P_{33}^{(1)}(\Omega,\Omega')=6\mu\mu'\cos\psi,\ P_{33}^{(2)}(\Omega,\Omega')=\tfrac{3}{2}(1-\mu^2)(1-\mu'^2)\cos2\psi.$$

We note that, just as in ordinary radiation transport theory, it is impossible to obtain from (6) equations that contain only the intensities $I^{(\beta)}(z,\Omega)$. In fact, even in the simplest case of normal incidence of unpolarized light on a crystal boundary, Eqs. (6) constitute a coupled system for the five quantities $I_l^{(1)}$, $I_r^{(1)}$, $I_l^{(2)}$, $I_r^{(2)}$, and $I^{(3)}$.

At the chosen normalization of the matrices $\mathbf{P}_{\beta\beta'}$ the expressions for the scattering coefficients and for the absorption coefficients take the form

$$a_{\beta\beta'}=\frac{2\pi}{\hbar}\cdot\frac{2}{3}V_0^2\frac{g_\beta(\omega)}{v_{\beta'}(\omega)}N_i s_\beta(\omega)s_{\beta'}(\omega),$$
$$\alpha_\beta=\frac{s_\beta}{v_\beta\tau_0}+\sum_{\beta'}\frac{h_{\beta'}}{2}a_{\beta'\beta}. \tag{15}$$

Here N_i is the impurity density, $g_\beta(\omega)=k_\beta^2/2\pi^2\hbar v_\beta$ is the state density of the polaritons of the branch β (without allowance for the double degeneracy of the transverse branches), $\mathbf{k}_\beta$ is the wave vector of the polariton at the frequency ω, and τ_0 is the nonradiative lifetime of the exciton. The strength function

$$s_{1,2}=\frac{\omega_{LT}\omega_0}{\omega_{LT}\omega_0+2[\omega_0(k_\beta)-\omega]^2},\quad s_3=1 \tag{16}$$

characterizes the fraction of the exciton component in the polariton.[10] We note that if we neglect the opto-exciton interaction ($\omega_{LT}=0$) we have for the exciton branch $s_\beta=1$ and $v_\beta=\hbar k/M$, and the reciprocal momentum relaxation time of the exciton is

$$\frac{1}{\tau_p^{(0)}}=\frac{2\pi}{\hbar}g_0V_0^2N_i,$$

where $g_0=Mk/2\pi^2\hbar^2$.

In addition to the already indicated conditions for the applicability of the transport equations (6), it was also assumed in the derivation of these equations that at $\omega>\omega_L$

$$k_\beta\gg\alpha_\beta\quad(\beta=1,2,3),$$
$$|k_\beta-k_{\beta'}|\gg\alpha_\beta,\ \alpha_{\beta'}\quad(\beta\neq\beta'), \tag{17}$$

and at $\omega<\omega_L$

$$k_1\gg\alpha_1,$$
$$|k_{2,3}|\gg\alpha_1. \tag{18}$$

Here $\omega_L=\omega_3(0)$ is the frequency of the longitudinal exciton at $k=0$. The first of the inequalities (17) or (18) is the usual criterion for the applicability of the kinetic equation, upon satisfaction of which the wave vector of the polariton is a well defined quantum number. This criterion leads, in particular to the inequality $\omega_{LT}\gg 1/\tau_p^{(0)}$, which is the opposite of the criterion proposed in Ref. 1. The second of the inequalities in (17) means that the correlation between the polaritons of the two branches $\beta=\beta'$ vanishes over the mean free path α_β^{-1} or $\alpha_{\beta'}^{-1}$, and the monochromatic field of the radiation propagating in the Ω direction is described by the matrices $\mathbf{I}^{(\beta)}(\Omega)$ ($\beta=1$, 2, 3), i.e., by nine scalar quantities. If the second of the inequalities in (17) were not satisfied, it would be necessary to introduce in addition components that characterize the correlation between polaritons from different branches. The second inequality of

(18) allows us to disregard, at frequencies below the longitudinal frequency ω_L, the spatially damped (even in the absence of exciton damping) waves 2 and 3 in the transport of the radiation in the crystal. This leaves in Eq. (6) only the quantity $I^{(1)}$. In the vicinity of the longitudinal frequency, the dispersion relation for the wave 2 can be approximately written in the form

$$\omega_2(k)=\omega_L+\hbar k^2/2\overline{M},$$
$$\frac{1}{\overline{M}}=\frac{1}{M}+\frac{1}{M_0},\quad M_0=\frac{\hbar\varepsilon_0}{2\omega_{LT}}\left(\frac{\omega_0}{c}\right)^2. \tag{19}$$

In this case the second condition of (18) is transformed into

$$[2\overline{M}(\omega_L-\omega)/\hbar]^{1/2}\gg\alpha_1.$$

Thus, the frequency region near ω_L is excluded from consideration.

We introduce a matrix S that connects the parameters of the secondary and incident fluxes in the absence of reflection from the internal boundary of the crystal[1]:

$$\mathbf{I}^{(\beta)}(0,\Omega)=\frac{1}{4\pi\mu}\sum_{\beta'}\int_{\mu'>0}d\Omega'\mathbf{S}_{\beta\beta'}(\Omega,\Omega')\mathbf{I}^{(\beta')}(0,\overline{\Omega}'). \tag{20}$$

Generalizing the method used in Ref. 11 of deriving the equation for the S matrix from the invariance principle, we obtain, taking into account the presence of several branches, the system of equations

$$\left(\frac{\alpha_\beta}{\mu}+\frac{\alpha_{\beta_0}}{\mu_0}\right)\mathbf{S}_{\beta\beta_0}(\Omega,\Omega_0)=\mathbf{G}_{\beta\beta_0}(\Omega,\Omega_0)$$
$$+\sum_{\beta'}\int_{\mu'>0}\frac{d\Omega'}{4\pi\mu'}\mathbf{S}_{\beta\beta'}(\Omega,\Omega')\mathbf{G}_{\beta'\beta_0}(\overline{\Omega}',\Omega_0), \tag{21}$$
$$\mathbf{G}_{\beta\beta'}(\Omega,\Omega')=a_{\beta\beta'}\mathbf{P}_{\beta\beta'}(\Omega,\overline{\Omega}')$$
$$+\sum_{\beta''}\int_{\mu''>0}\frac{d\Omega''}{4\pi\mu''}a_{\beta\beta''}\mathbf{P}_{\beta\beta''}(\Omega,\Omega'')\mathbf{S}_{\beta''\beta'}(\Omega'',\Omega').$$

We introduce next the matrix $\mathbf{S}^R_{\beta\beta}$, which connects the quantities $\mathbf{I}^{(\beta)}(0,\Omega)$ and $\mathbf{I}^{(\beta')}(0,\Omega)$ on the inner surface of the crystal ($z=+0$), with account taken of the reflection from the boundary. The system of equations for the $\mathbf{S}^R_{\beta\beta'}$ matrices is a natural generalization of the equation [see (17) of Ref. 1]

$$\mathbf{S}^R_{\beta\beta'}(\Omega,\Omega_0)=\mathbf{S}_{\beta\beta'}(\Omega,\Omega_0)$$
$$+\sum_{\beta_1,\beta_2}\int_{\mu'>0}\frac{d\Omega'}{4\pi\mu'}\mathbf{S}_{\beta\beta_1}(\Omega,\overline{\Omega}')\mathbf{R}_{\beta_1\beta_2}(\mu')\mathbf{S}^R_{\beta_2\beta'}(\Omega',\Omega_0), \tag{22}$$

where $\mathbf{R}_{\beta_1\beta_2}(\mu')$ is the matrix of the reflection coefficients, $\overline{\Omega}'$ and Ω' are connected by the relation $n^2_{\beta_1}(1-\overline{\mu}'^2)=n^2_{\beta_2}(1-\mu'^2)$, and $\overline{\varphi}'=\varphi'$.

In analogy with Ref. 1, we designate the unit vector in the direction of propagation of the wave incident in vacuum on the crystal by $\overline{\Omega}_1=(-\mu_1,\ \varphi_1)$, in the direction of propagation of the initial wave refracted in the crystal by $\overline{\Omega}_{0\beta}=(-\mu_{0\beta},\ \varphi_{0\beta})$, in the direction of propagation of the diffusely reflected wave incident on the inner boundary of the crystal by $\Omega_\beta=(\mu_2,\ \varphi_2)$, and in the direction of propagation of the wave emerging from the crystal by $\Omega_2=(\mu_2,\ \varphi_2)$. In this case $\varphi_{0\beta}=\varphi_1$, $\varphi_\beta=\varphi_2$, and $\mu_{0\beta}$ and μ_1 or μ_β and μ_2 are connected by Snell's relation

$$(1-\mu_1^2)=n_\beta^2(1-\mu_{0\beta}^2),\quad (1-\mu_2^2)=n_\beta^2(1-\mu_\beta^2). \tag{23}$$

The matrix $\mathbf{S}^H(\Omega_2,\ \Omega_1)$, which determines the connection between the scattered radiation outside the crystal $\mathbf{I}(-0,\ \Omega_2)$ with the flux $\pi\mathbf{F}(-0,\ \overline{\Omega}_1)$ incident on the crystal

$$\mathbf{I}(-0,\Omega_2)=\frac{1}{4\mu_2}\mathbf{S}^H(\Omega_2,\Omega_1)\mathbf{F}(-0,\overline{\Omega}_1), \tag{24}$$

is connected with the matrix $\mathbf{S}^R_{\beta\beta'}$ by the relation

$$\mathbf{S}^H(\Omega_2,\Omega_1)=\sum_{\beta,\beta'}\mathbf{T}_{0\beta}(\mu_2,\mu_\beta)\mathbf{S}^R_{\beta\beta'}(\Omega_\beta,\Omega_{\beta'})$$
$$\times\mathbf{T}_{\beta'0}(\mu_{0\beta'},\mu_1)\frac{\mu_2\mu_1}{\mu_\beta\mu_{0\beta'}}\frac{1}{n_\beta^2},$$

where $\mathbf{T}_{\beta 0}$ and $\mathbf{T}_{0\beta}$ are the transmission matrices from the vacuum into the crystal and from the crystal into the vacuum, and $n_\beta=ck_\beta/\omega$. Equation (24) is a generalization of Eq. (48) of Ref. 1.

We calculate first the frequency dependence of the intensity and of the degree of polarization of the scattered radiation in the absence of spatial dispersion, when $M\to+\infty$. We consider next the radiation transport at a finite effective mass of the exciton, when additional light waves must be taken into account.

§3. RADIATION TRANSPORT IN THE ABSENCE OF SPATIAL DISPERSION

As $M\to\infty$ the frequency of the mechanical exciton is independent of the wave vector, i.e., $\omega_0(k)\equiv\omega_0$, and each pair of values $\Omega=\mathbf{k}/k$ and ω in the frequency region

$$\omega<\omega_0\quad\text{or}\quad\omega>\omega_L \tag{25}$$

corresponds, just as under nonresonant conditions, to two normal (transverse) waves (Fig. 1a). According to (1) and (2), the refractive index and the group velocity of these waves are

$$n(\omega)=\frac{ck}{\omega}=n_0\left(\frac{\omega_L-\omega}{\omega_0-\omega}\right)^{1/2},\quad v(\omega)=\frac{c}{n(\omega)}\left[1+\frac{\omega\omega_{LT}}{2(\omega_0-\omega)(\omega_L-\omega)}\right]^{-1} \tag{26}$$

where $n_0=\varepsilon_0^{1/2}$. In the region of the residual rays, $\omega_0<\omega<\omega_L$, the volume waves are not excited, and we shall not consider in the present section. We note that in the frequency range from ω_0 to $\omega_s=\omega_L-[\omega_{LT}/(\varepsilon_0+1)]$, the diffuse scattering can result from optical excitation and emission (with participation of the impurities) of surface polaritons. In this case the problem reduces to two-dimensional radiation transport by surface polaritons with wave vector

$$k_*=\frac{\omega}{c}\left[\frac{\varepsilon(\omega)}{\varepsilon(\omega)+1}\right]^{1/2}$$

and with coefficient of attenuation in the interior of the crystal (see, e.g., Ref. 12)

$$\varkappa_*=\frac{\omega}{c}\left[-\frac{\varepsilon^2(\omega)}{\varepsilon(\omega)+1}\right]^{1/2}. \tag{27}$$

At $\omega_0<\omega<\omega_s$ the dielectric constant is $\varepsilon(\omega)=n^2(\omega)<-1$. Thus, in the absence of spatial dispersion, at any ω from the region (25), the index β in the transport equation runs through only one value ($\beta=1$ at $\omega<\omega_0$ and $\beta=2$ at $\omega>\omega_L$), and can therefore be omitted. $\mathbf{S}^R$ is therefore a 4×4 matrix in this case, and is determined

completely by specifying two parameters: the refractive index n, which determines the reflection coefficient $\mathbf{R}$ [see Eq. (8) of Ref. 1], and the quantum yield $\tilde{\omega}_0$ in a single scattering act. The problem of finding this matrix reduces therefore to the problem solved in the preceding paper.[1] The only difference lies in the allowance for the frequency dependence of the refractive index, which is determined by formula (26), and in the more complicated frequency dependence of the quantum yield for one scattering act

$$\tilde{\omega}_0=\tau/\tau_p=(1+\tau_p/t_0)^{-1}. \tag{28}$$

Here $\tau=(\tau_p^{-1}+t_0^{-1})^{-1}$ is the total lifetime of the polariton in a state with a specified momentum, $\tau_p=(va_{BB})^{-1}$ is the polariton momentum relaxation time, $t_0(\omega)=s^{-1}(\omega)\tau_0$ is its lifetime, and τ_0 is the lifetime of the mechanical exciton, which we regard as a constant. Using (15) and (16) we obtain for the ratio t_0/τ_p that determines the value of $\tilde{\omega}_0$,

$$\frac{t_0}{\tau_p}=\frac{1}{3\pi}N_i V_0^2\frac{\tau_0 k_0^2 n_0^2}{\hbar^2 c}n(\omega)\frac{\omega_{LT}\omega_0}{(\omega_0-\omega)^2}, \tag{29}$$

where $k_0=\omega_0/c$. According to (28) and (29), the function $\tilde{\omega}_0(\omega)$ is completely specified if ω_L and ω_0 are given, provided that the value of $\tilde{\omega}_0$ for some single value of ω is known. In the calculation we have specified the value of $\tilde{\omega}_0$ at $\omega=\omega_0-(\omega_{LT}/2)$, which we shall henceforth designate by $\tilde{\omega}_0'$.

The matrix $\mathbf{S}^R$ was calculated by the previously described method.[1] Figures 2 and 3 show the frequency dependences of the intensity and of the degree of linear polarization of the radiation scattered in the direction $\mu_2\approx 1$ under normal excitation ($\mu_1=1$) by linearly polarized light; these dependences were calculated, without allowance for the spatial dispersion, for different values of $\tilde{\omega}_0'$ at $\varepsilon_0=n_0^2=8.3$.

The behavior of the plots in Figs. 2 and 3 can be understood by determining the influence of a change of $\tilde{\omega}_0$ or of n on the intensity and polarization of the scattered radiation. With increasing $\tilde{\omega}_0$, the probability of nonradiative recombination of the polariton decreases and

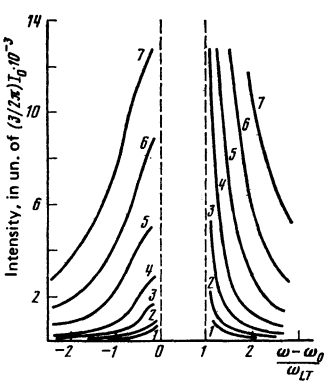

FIG. 2. Frequency dependence of the intensity of the backscattered radiation at normal excitation (in the absence of spatial dispersion). Curves 1—7 pertain to different values of the lifetime of the exciton, corresponding to the following values of the quantum yield for a unit act of polariton scattering at the frequency $\omega=\omega_0-(\omega_{LT}/t)$: 0.1 (curve 1); 0.2 (2); 0.4 (3); 0.6 (4); 0.8 (5); 0.9 (6), and 0.95 (7); $n_0^2=8.3$.

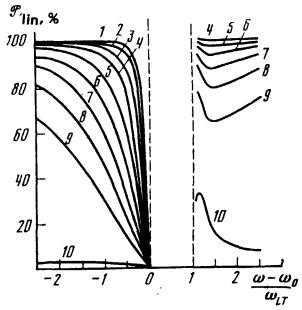

FIG. 3. Dependence of $\mathscr{P}_{\text{lin}}(\omega)$ under normal excitation by linearly polarized light in the absence of spatial dispersion. The parameters used in the calculation of curves 1—7 are the same as in Fig. 2. Curves 8—10 were calculated at $\tilde{\omega}'_0$ equal to 0.975 (8), 0.99 (9), and 1.0 (10).

the radiation intensity increases. The degree of polarization should in this case decrease, since an increase of $\tilde{\omega}_0$ leads to an increase in the average number $\bar{N}$ of the scattering acts experienced by a polariton that reaches the boundary and is emitted into the vacuum. With increasing $|n-1|$, the number of scattering acts due to specular reflection by the inner surface of the crystal also increases.[2)] This leads to a decrease of the degree of polarization of the radiation, and at $\tilde{\omega}_0 \neq 1$ also to a decrease of the intensity.

According to (20) and to Eq. (21) of Ref. 1, under normal excitation by linearly polarized light we have for the backscattered radiation

$$I(-0,1)\equiv I(z=-0,\mu_2\approx 1)=\frac{T^2(1)}{4n^2}(S_{11}^R+S_{21}^R)F,$$
$$\mathscr{P}_{\text{lin}}=(S_{11}^R-S_{21}^R)/(S_{11}^R+S_{21}^R), \tag{30}$$

where $T(1)=4n/(1+n)^2$.

At $\tilde{\omega}_0\ll 1$ we have $S_{11}^R=c_{11}^{(1)}\tilde{\omega}_0$ and $S_{21}^R=C_{21}^{(2)}\tilde{\omega}_0^2$, inasmuch as in single scattering we have $S_{ij}^R\sim P_{11,ij}$, and $c_{21}^{(1)}=0$. Consequently, at $\tilde{\omega}_0\ll 1$ we have

$$I(-0,1)\sim\tilde{\omega}_0/(1+n)^4,\quad \mathscr{P}_{\text{lin}}=1-2c_{21}^{(2)}\tilde{\omega}_0/c_{11}^{(1)}. \tag{31}$$

We note that the coefficient $c_{11}^{(1)}$ does not depend on the refractive index n. At $n\gg 1$ or $n\ll 1$ the coefficient $c_{21}^{(2)}$ is likewise practically independent of n.

The quantum yield $\tilde{\omega}_0$ at $\omega<\omega_0$ increases monotonically with increasing ω, reaching unity as $\omega\to\omega_0$. Since in the frequency region $\omega_0-\omega\gg\omega_{LT}$ we have $\tilde{\omega}_0\to 0$, we get with decreasing frequency $I(-0,1)\to 0$ and $\mathscr{P}_{\text{lin}}\to 1$. In the frequency region close to ω_0, such that $n\gg 1$ but still $\tilde{\omega}_0\ll 1$, the intensity $I(-0,1)\sim(\omega_0-\omega)^{-1/2}$. As $\omega\to\omega_0$, saturation of $\tilde{\omega}_0$ sets in, the refractive index increases without limit, and $T(1)|_{\omega=\omega_0}\sim(\omega_0-\omega)^{1/2}$. Since $T(1)(S_{11}^R+S_{21}^R)/n^2$, just as the total quantum yield, remains bounded, at sufficiently small values of $\omega_0-\omega$ the function $I(-0,1;\omega)$ reaches a maximum and begins to decrease. In the scale of Fig. 2, one cannot see the decrease of $I(-0,1)$, and only a tendency to saturation is observed. The monotonic increase of $\tilde{\omega}_0$ and of n with increasing ω in the region $\omega<\omega_0$ leads to a monotonic decrease of $\mathscr{P}_{\text{lin}}$. As $\omega\to\omega_0$, for any value of $\tilde{\omega}_0'$ at the frequency $\omega_0-(\omega_{LT}/2)$ the average number of scattering acts $\bar{N}\to\infty$ and $\mathscr{P}_{\text{lin}}\to 0$.

At $\omega\geq\omega_L$, the quantum yield $\tilde{\omega}_0$ increases from zero

at $\omega=\omega_L$, reaches a maximum value $\tilde{\omega}_{0M}$ at $\omega_M=\omega_L+(\omega_{LT}/4)$, and then again decreases to zero. The value of t_0/τ_p at the maximum point ω_M is smaller by a factor $25\sqrt{15}/4$ than at $\omega=\omega_0-(\omega_{LT}/2)$. Therefore, whereas at the frequency $\omega_0-(\omega_{LT}/2)$ the ratio $t_0/\tau_p\leqslant 1$, i.e., $\omega_0'\leqslant 1/2$, at $\omega>\omega_L$ we have $\tilde{\omega}_0\approx t_0/\tau_p\ll 1$. At ω close to ω_L, the intensity $I(-0,\ 1)\sim n/(1+n)^4$. Therefore as $\omega\to\omega_L$ the function $I(-0,\ 1)$ increases, reaches a maximum at the frequency $\omega_L+[\omega_{LT}/(9\varepsilon_0-1)]$, and then decreases. The region of the decrease of $I(-0,\ 1)$ as $\omega\to\omega_L$ cannot be seen in the scale of Fig. 2.

Curve 10 of Fig. 3 was calculated for the case when $\tilde{\omega}_0=1$ in the entire considered frequency interval. In this case the function $\mathscr{P}_{1\text{in}}(\omega)$ has a maximum at the point $\omega_1=\omega_L+\omega_{LT}/(\varepsilon_0-1)$, where $n=1$. When a deviation from this frequency takes place towards the right or towards the left, reflection by the boundary comes into play and $\mathscr{P}_{1\text{in}}$ decreases. In the case when the quantum yield $\tilde{\omega}_0'$ differs from unity and therefore the function $\tilde{\omega}_0(\omega)$ depends strongly on the frequency, the frequency dependence of $\mathscr{P}_{1\text{in}}(\omega)$ has a more complicated form. At $\omega_1<\omega<\omega_M$ the increase of the frequency leads to an increase of $\tilde{\omega}_0$ and of n. Therefore, when ω increases from ω_1 to ω_M the degree of polarization $\mathscr{P}_{1\text{in}}$ decreases steeply and assumes a minimum value near ω_M. Near the frequency ω_1 is located the inflection point of the $\mathscr{P}_{1\text{in}}(\omega)$ curve. The region of small values of $\omega-\omega_L$, where $\mathscr{P}_{1\text{in}}\to 1$, cannot be seen in the scale of Fig. 3. The value $\tilde{\omega}_0'$ at which the transition from curves of type 10 to curves of type 1–9 in Fig. 3 takes place is close to unity. Thus, curve 9 corresponds to a value $1-\tilde{\omega}_0'=0.01$, which corresponds to $t_0/\tau_p=99$ at the frequency $\omega_0-\omega_{LT}/2$.

§4. RADIATION TRANSPORT IN THE PRESENCE OF SPATIAL DISPERSION

The analysis of radiation transport in the regions $\omega<\omega_L$ and $\omega>\omega_L$ in the presence of spatial dispersion calls for a different approach.

a) The case $\omega<\omega_L$

Inasmuch as at $\omega<\omega_L$ we have $|k_2|=(\omega/c)[-\varepsilon(\omega,k_2)]^{1/2}$ and in the frequency region $\omega_0<\omega<\omega_s$ we have $\varepsilon(\omega,\ 0)<-1$, the surface-polariton damping coefficient is, according to (27), $\varkappa_s(M\to\infty)>|k_2|$. Therefore when the condition $|k_2|\gg\alpha_1$ is satisfied the principal contribution to the radiation is made by volume waves of the branch 1, and there is no need to include into consideration the energy transport by the surface waves.[3)] Thus, at $\omega<\omega_L$ the transport equation takes the same form as in Ref. 1. In contrast to Ref. 1 or to the case $M=\infty$ considered above, when calculating the reflection-coefficient matrix $\mathbf{R}_{11}(\mu)$ for wave 1 it is necessary to take into account also waves 2 and 3, which have at $\omega<\omega_L$ an imaginary wave vector (Fig. 1b). It is known that in this case it is necessary to specify, besides the Maxwell boundary conditions, also additional boundary conditions (ABC). We used the ABC proposed by Pekar,[15]

$$\mathbf{P}|_{z=0}=0, \tag{32}$$

where $\mathbf{P}(z,\omega)$ is the exciton contribution to the polarization of the medium.

The matrix $\mathbf{R}_{11}(\mu)$ can be represented in the form [Eq. (8) of Ref. 1]

$$\mathbf{R}_{11}(\mu)=\begin{bmatrix} R_1 & 0 & 0 & 0\\ 0 & R_2 & 0 & 0\\ 0 & 0 & R_3 & -R_4\\ 0 & 0 & R_4 & R_3\end{bmatrix}, \tag{33}$$

where $R_1=|r_p|^2$, $R_2=|r_s|^2$, $R_3=\mathrm{Re}(r_pr_s^*)$, and $R_4=\mathrm{Im}(r_pr_s^*)$. Here r_p and r_s are the maximum amplitudes of the reflection coefficients in the p and s components, respectively. It is convenient to express these coefficients in terms of the effective refractive indices $\bar{n}_p$ and $\bar{n}_s$:

$$r_p=\frac{1-\bar{n}_p}{1+\bar{n}_p},\quad r_s=-\frac{1-\bar{n}_s}{1+\bar{n}_s}. \tag{34}$$

Under the ABC (32), $\bar{n}_p$ and $\bar{n}_s$ take the form

$$\begin{aligned}\bar{n}_p(\mu)=\frac{n_1^2}{n_{1z}}&\left[n_{0z}(n_{2z}n_{3z}+n_1^2(1-\mu^2))-n_2^2\frac{n_1^2-\varepsilon_0}{n_2^2-\varepsilon_0}\left(n_{0z}+\frac{n_{2z}}{\varepsilon_0}\right)(1-\mu^2)\right]\\ &\times\left[n_{2z}n_{3z}\frac{n_1^2-n_2^2}{\varepsilon_0-n_2^2}-n_{0z}n_{3z}n_2^2\frac{n_1^2-\varepsilon_0}{n_2^2-\varepsilon_0}+\frac{n_1^4}{\varepsilon_0}(1-\mu^2)\right]^{-1},\\ \bar{n}_s(\mu)=&\frac{n_{1z}(\varepsilon_0-n_2^2)}{n_{0z}(n_1^2-n_2^2)+n_{2z}(n_1^2-\varepsilon_0)}.\end{aligned} \tag{35}$$

The wave refractive index is here $n_\beta=ck_\beta/\omega$ and $n_{1z}n_1\mu$, while the quantities n_{0z} and $n_{\beta z}$ ($\beta=2,\ 3$) are obtained from the condition of conservation of the tangential components of the wave vector

$$n_{0z}=[1-n_1^2(1-\mu^2)]^{1/2},\quad n_{\beta z}=[n_\beta^2-n_1^2(1-\mu^2)]^{1/2}. \tag{36}$$

At $\omega<\omega_L$ both n_2^2 and n_3^2 are negative. We note that there is no need to take into account the exciton damping in the calculation of $\mathbf{R}_{11}(\mu)$, since this would be an exaggeration of the accuracy with respect to the small parameters corresponding to the conditions (18). Expressions (35) determine also the effective refractive indices n_p and n_s that describe the maximum amplitudes of the reflection coefficients of light from vacuum, and they can be reduced to the form obtained in Refs. 15–17. The fact that the corresponding "vacuum–crystal" and "crystal–vacuum" reflection coefficients coincide at $\omega<\omega_L$ is the consequence of the time-reversal symmetry. Unlike in the Refs. 15–17, formulas (35) are valid in the entire interval $0<\theta<\pi/2$ of the angle of incidence of the wave 1 on the crystal boundary.

According to (35), with allowance for the spatial dispersion, a change of the linear polarization into circular and vice versa upon specular reflection takes place not only at angles θ larger than the total internal reflection angle $\theta_0=\sin^{-1}(1/n_1)$, but also at $\theta<\theta_0$.

The transmission-coefficient matrix $\mathbf{T}_{11}(\mu)$ has likewise a more complicated form than the matrix $\mathbf{T}$ in Eq. (11) of Ref. 1. If it is represented in a form similar to (33), introducing the quantities $T_i(\mu)$ ($i=1-4$), then we obtain

$$\begin{aligned}&T_1=1-R_1,\quad T_2=1-R_2,\\ &T_3=\frac{n_{0z}}{\mu n_1}\frac{w_0}{w_1}\mathrm{Re}(t_pt_s^*),\quad T_4=\frac{n_{0z}}{\mu n_1}\frac{w_0}{w_1}\mathrm{Im}(t_pt_s^*),\end{aligned} \tag{37}$$

where

$$t_p=\frac{2\bar{n}_p}{1+\bar{n}_p}\left(n_1-n_2\frac{n_1^2-\varepsilon_0}{n_2^2-\varepsilon_0}\frac{n_1^2(1-\mu^2)-n_{1z}n_{3z}/\bar{n}_p}{n_{2z}n_{3z}+n_1^2(1-\mu^2)}\right) \tag{38}$$

$$t_s=\frac{2\bar{n}_s}{1+\bar{n}_s}\frac{n_1^2-n_2^2}{\varepsilon_0-n_2^2},$$

$\bar{n}_p$ and $\bar{n}_s$ are the effective refractive indices (35), and

$$w_0=\frac{c}{8\pi},\quad w_1=\frac{c}{8\pi}\left[1+\left(\frac{n_1^2}{n_0^2}-1\right)^2\frac{M_0}{M}\right].$$

Taking into account the spatial dispersion, the frequency dependence of the ratio of the polariton lifetime t_{01} to its momentum relaxation time τ_{p1} becomes smoother and takes the form

$$\frac{t_{01}}{\tau_{p1}}=\frac{1}{3\pi}V^2N_i\frac{k_0^2\tau_0 n_0^2}{\hbar^2 c}\frac{\omega_{LT}\omega_0 n_1(\omega)}{[\omega_0(k_1)-\omega]^2+M_0\omega_{LT}^2/M}. \tag{39}$$

As $M\to\infty$, Eq. (39) goes over into (29), as it should.

The theoretical plots of $I(-0,\ 1;\ \omega)$ and $\mathscr{P}_{1\text{in}}(\omega)$ in Figs. 4 and 5 in the frequency region $\omega<\omega_L$ were calculated for $M=m_0$ (m_0 is the mass of the free electron), $\hbar\omega_0=2.552$ eV, $\hbar\omega_{LT}=2.0$ meV, and $\varepsilon_0=8.3$. In the calculation we used the same set of values of $V_0^2N_i\tau_0$ as in Fig. 2. However, when account is taken of the finite mass $M<+\infty$, the values of $\tilde{\omega}_0'$ are somewhat decreased to 0.07 (curve 1), 0.14 (2), 0.32 (3), 0.50 (4), 0.73 (5), 0.86 (6), and 0.93 (7).

On the long-wave section of the spectrum, i.e., at $\omega_0-\omega<\omega_{LT}$, the spatially damped waves 2 and 3 have little effect on the reflection-coefficient matrix, and the functions $I(-0,\ 1,\ \omega)$ and $\mathscr{P}_{1\text{in}}(\omega)$ are close to the analogous functions calculated without allowance for spatial dispersions.

The frequency dependences of Fig. 5 can be explained by using the results of Ref. 1. It was shown there that the degree of polarization of the radiation in the $\mu_1=1$ and $\mu_2\approx 1$ geometry is practically independent of n if the following inequality holds

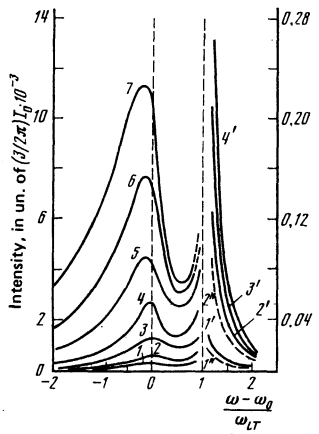

FIG. 4. Frequency dependence of the intensity of secondary radiation in the presence of spatial dispersion. The effective exciton mass M was assumed equal to the mass of the free electron. In the calculation in the frequency region $\omega<\omega_L$ (left-hand scale) we used the same values of τ_0, $V_0^2N_i$, n_0^2, $\hbar\omega_0=2.552$ eV, and $\hbar\omega_{LT}=2$ meV as in Fig. 2. The curves in the region $\omega>\omega_L$ (right-hand scale) were calculated with $\tilde{\omega}_0$ having at the frequency $(\omega_L+0.15\ \omega_{LT})$ the values 0.135 (curves 1′, 1″), 0.607 (2′, 2″), 0.824 (3′), and 1.0 (4′). The curves 1″ and 2″ describe the contribution of the polaritons of only the upper polariton branch 2.

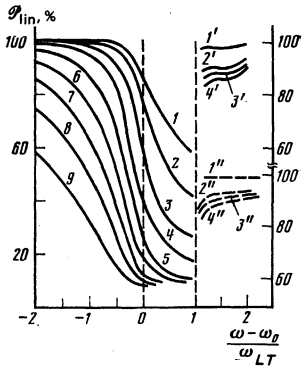

FIG. 5. Plot of $\mathscr{P}_{\text{lin}}(\omega)$ under normal excitation by linearly polarized light with allowance for the spatial dispersion. The parameters are the same as in Fig. 4. Curves 1′–4′ were calculated with allowance for the longitudinal waves, and curves 1″–4″ without allowance for the longitudinal waves.

$$1-\bar{R}\ll 1-\eta_0(\tilde{\omega}_0,\ 1), \tag{40}$$

where $\eta_0(\tilde{\omega}_0,\ 1)$ is the total quantum yield, i.e., the ratio of the outgoing flux to the incident flux in the absence of reflection from the boundary ($n=1$). This result is connected with the fact that the average number of reflections of the radiation prior to the emergence into the vacuum does not depend under the condition (40) on $\bar{R}$ and is close to $[1-\eta_0(\tilde{\omega}_0,\ 1)]^{-1}$. If it is assumed approximately that the radiation approaching again the inner boundary of the crystal after specular reflection is not polarized, and the inequality (40) holds, then the degree of polarization with allowance for reflection from the boundary is

$$\mathscr{P}_{\text{lin}}(\omega)\approx\mathscr{P}_{\text{lin}}(\tilde{\omega}_0,\ 1)[1-\eta_0(\tilde{\omega}_0,\ 1)], \tag{41}$$

where $\mathscr{P}_{1\text{in}}(\tilde{\omega}_0,\ 1)$ is the degree of polarization at $n=1$. Figure 6 shows curves 4 and 7 of Fig. 4, as well as curves plotted in accordance with Eq. (41). This approximate formula holds so long as $\tilde{\omega}_0\leq 0.995$. At larger values of $\tilde{\omega}_0$, the approximations used in the derivation of (41) are no longer satisfied. Therefore the exact and approximate values of $\mathscr{P}_{1\text{in}}$ differ significantly for curve 7 at $\omega=\omega_0+(\omega_{LT}/2)$, where $\tilde{\omega}_0=0.9977$.

Under the assumption indicated above, the expression

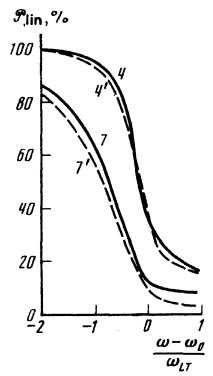

FIG. 6. Comparison of the results of the exact and approximate calculations for $\mathscr{P}_{\text{lin}}(\omega)$. Curve 3, 7—the same as in Fig. 4, curves 4′ and 7′ were calculated from the approximate formula (41).

for the intensity takes the simple form

$$I(-0,1;\omega)\approx\frac{T^2(1)}{n_1^2}\frac{\eta_0(\tilde\omega_0,1)}{1-\eta_0(\tilde\omega_0,1)}F, \tag{42}$$

where πF is the flux incident on the crystal. Formula (42) accounts well for the frequency dependence of $I(-0, 1)$ in the region $\omega<\omega_L$. The maximum of $I(-0, 1)$ in the region of the frequency ω_0 (see Fig. 4) is due to the increase of $\tilde\omega_0$ with increasing frequency. In the region of the longitudinal-transverse splitting, the quantity $\eta_0(\tilde\omega_0, 1)$ increases with increasing frequency, and $T^2(1)/n_1^2$ goes through a gently sloping minimum and then increases smoothly, reaching at $\omega=\omega_L$ the value $16\varepsilon_0^2/(n_1+\varepsilon_0)^4$. It is this which causes the second growth of $I(-0, 1; \omega)$ as $\omega\to\omega_L$.

At $n^2\gg1$ the solid angle $\Delta\Omega\approx\pi/n^2$ in which the radiation can emerge from the crystal to the vacuum is very small, and within this solid angle one can certainly neglect the angular dependence of the intensity. Therefore the angular dependence of the outgoing radiation duplicates with high accuracy the angular dependence of the transmission coefficient

$$\mathbf{I}(-0,\mu_2,\varphi)\approx\frac{1}{n^2}\mathbf{T}(\mu)\mathbf{I}(+0,\mu=1,\varphi). \tag{43}$$

In the present paper we assume that the boundary is ideal and do not take into account the scattering of the light by the surface roughnesses. Since in scattering of light by surface roughnesses the angular dependence of the intensity of the scattered radiation differs in general from (43), it becomes possible to distinguish experimentally between diffuse scattering effects in the volume and on the boundary.

b) Case $\omega>\omega_L$

Under the assumptions made above, the total quantum yield for one polariton scattering act

$$\tilde\omega_{0,\beta}=\frac{\tau_{p\beta}^{-1}}{t_{0\beta}^{-1}+\tau_{p\beta}^{-1}}=\sum_{\beta'}h_{\beta'}a_{\beta'\beta}/2\alpha_\beta$$

does not depend on the number of the polariton branch. The ratio of the lifetime of the polariton to the momentum relaxation time is in this case

$$\frac{t_{0\beta}}{\tau_{p\beta}}=\frac{2\pi}{3}V_0^2N_i\frac{\tau_0}{\hbar}\sum_{\beta'}h_{\beta'}s_{\beta'}(\omega)g_{\beta'}(\omega). \tag{44}$$

The scattering coefficients satisfy the relation

$$a_{\beta\beta'}a_{\beta'\beta''}=a_{\beta\beta''}a_{\beta'\beta'}, \tag{45}$$

which follows from the expression (15) for $a_{\beta\beta'}$. This property of the scattering coefficients, together with the possibility of factorizing the matrices $\mathbf{P}_{\beta\beta'}(\Omega,\Omega')$ [see (11)] allow us to write down the general solution of the system of equations for the $\mathbf{S}_{\beta\beta'}$ matrices in the form

$$\mathbf{S}_{\beta\beta'}(\Omega,\Omega')=a_{\beta\beta'}(\alpha_\beta/\mu+\alpha_{\beta'}/\mu')^{-1}\mathbf{U}_\beta\Theta_\beta(\Omega)\mathbf{H}_\beta(\mu)\tilde{\mathbf{H}}_{\beta'}(\mu')\Theta_{\beta'}^+(\Omega')\mathbf{U}_{\beta'}^{-1}, \tag{46}$$

where $\mathbf{H}_\beta(\mu)$ are 9×9 matrices.

Substituting (46) in (21), we obtain after simple transformations the equation that the matrix $\mathbf{H}_\beta(\mu)$ satisfies,

$$\mathbf{H}_\beta(\mu)=1+\mu\mathbf{H}_\beta(\mu)\sum_{\beta'}\int_0^1 d\mu'\frac{a_{\beta\beta'}}{\alpha_\beta\mu'+\alpha_{\beta'}\mu}\tilde{\mathbf{H}}_{\beta'}(\mu')\Psi_{\beta'}(-\mu'), \tag{47}$$

where

$$\Psi_\beta(\mu)=\frac{3}{8\pi}\int_0^{2\pi}d\varphi\,\Theta_\beta^+(\Omega)\Theta_\beta(\Omega).$$

The matrix Ψ_β is determined only by the multiplicity of the degeneracy of the branch β. By the unitary transformation $D^{-1}\Psi_\beta(\mu)D$ with

$$\mathbf{D}=\begin{bmatrix}\Sigma_1&0&0&0&0\\0&1&0&0&0\\0&0&\Sigma_2&0&0\\0&0&0&\Sigma_2&0\\0&0&0&0&\Sigma_2\end{bmatrix},\quad \Sigma_1=\frac{1}{\sqrt2}\begin{bmatrix}1&1\\-1&1\end{bmatrix},\quad \Sigma_2=\frac{1}{\sqrt2}\begin{bmatrix}1&1\\1&-1\end{bmatrix},$$

the matrix $\Psi_\beta(\mu)$ reduces to a quasidiagonal matrix containing one 2×2 block

$$\Psi_\beta^{(0)}(\mu)=\tfrac{3}{4}\tilde{\mathbf{m}}_\beta(\mu)\mathbf{m}_\beta(\mu) \tag{48}$$

and four different functions

$$\begin{aligned}
\Psi_{v,\beta}^{(0)}(\mu)&=\begin{cases}\tfrac{3}{4}\mu^2 & (\beta=1,2),\\ 0 & (\beta=3)\end{cases}\\
\Psi_\beta^{(1)}(\mu)&=\begin{cases}\tfrac{3}{8}(1-\mu^2)(1+2\mu^2) & (\beta=1,2),\\ \tfrac{3}{4}\mu^2(1-\mu^2) & (\beta=3),\end{cases}\\
\Psi_{r,\beta}^{(1)}(\mu)&=\begin{cases}\tfrac{3}{8}(1-\mu^2) & (\beta=1,2),\\ 0 & (\beta=3),\end{cases}\\
\Psi_\beta^{(2)}(\mu)&=\begin{cases}\tfrac{3}{16}(1+\mu^2)^2 & (\beta=1,2),\\ \tfrac{3}{16}(1-\mu^2)^2 & (\beta=3).\end{cases}
\end{aligned} \tag{49}$$

On the diagonal, the function $\Psi_{v,\beta}^{(0)}(\mu)$ is contained once, and the remaining three functions twice. The matrix $\mathbf{m}_\beta(\mu)$ has the dimensionality $h_\beta\times2$ and coincides with the upper left-hand block $h_\beta\times2$ of the matrix $\mathbf{M}_\beta$ in (13). We note that the matrix

$$\begin{bmatrix}\Psi_\beta^{(0)}(\mu)&0&0\\0&0&0\\0&0&\Psi_{v,\beta}^{(0)}(\mu)\end{bmatrix}$$

coincides at $\beta=1$ or 2 with the matrix $\Psi^{(0)}(\mu)$ of Eq. (31) of Ref. 1, while the functions $\Psi_\beta^{(1)}(\mu)$, $\Psi_{r,\beta}^{(1)}(\mu)$, and $\Psi_\beta^{(2)}(\mu)$ with $\beta=1$ or 2 go over into the Ψ functions of Eq. (32a) of Ref. 1.

Thus, to determine the $\mathbf{S}_{\beta\beta'}$ matrices in the general case we must solve a system of three equations (47) for 2×2 matrices $\mathbf{H}_\beta^{(0)}(\mu)$, two systems of two equations (47) for the functions $H_{44,\beta}^{(0)}(\mu)$ and $H_{r,\beta}^{(1)}(\mu)$ with the functions $\Psi_{v,\beta}^{(0)}(\mu)$ and $\Psi_{r,\beta}^{(1)}(\mu)$, and two systems of three equations (47) for the functions $H_\beta^{(1)}(\mu)$ and $H_\beta^{(2)}(\mu)$ with the functions $\Psi_\beta^{(1)}(\mu)$ and $\Psi_\beta^{(2)}(\mu)$ in the integrand of (47). As a result we obtain for the S matrices

$$\begin{aligned}
\mathbf{S}_{\beta\beta'}(\Omega,\Omega')&=\tfrac{3}{4}\mathbf{S}_{\beta\beta'}^{(0)}(\mu,\mu')+[(1-\mu^2)(1-\mu'^2)]^{1/2}\\
&\times\mathbf{S}_{\beta\beta'}^{(1)}(\mu,\mu')\mathbf{P}_{\beta\beta'}^{(1)}(\Omega,\bar\Omega')+S_{\beta\beta'}^{(2)}(\mu,\mu')\mathbf{P}_{\beta\beta'}^{(2)}(\Omega,\bar\Omega').
\end{aligned} \tag{50}$$

The matrices $\mathbf{P}_{\beta\beta'}^{(1)}$ and $\mathbf{P}_{\beta\beta'}^{(2)}$ are defined here in accordance with (14),

$$\begin{aligned}
\mathbf{S}_{\beta\beta'}^{(0)}(\mu,\mu')&=\frac{a_{\beta\beta'}}{\alpha_\beta/\mu+\alpha_{\beta'}/\mu'}\mathbf{L}_\beta(\mu)\tilde{\mathbf{L}}_{\beta'}(-\mu'),\\
\mathbf{L}_\beta(\mu)&=\mathbf{M}_\beta(\mu)\begin{bmatrix}\mathbf{H}_\beta^{(0)}(\mu)&0\\0&H_{44,\beta}^{(0)}(\mu)\end{bmatrix}.
\end{aligned} \tag{51}$$

At $\beta,\beta'=1$, 2 the matrix $\mathbf{S}_{\beta\beta'}^{(1)}$, just as the matrix $\mathbf{S}^{(1)}$ in Ref. 1, is determined by two linearly independent functions

At $\beta=3$ or $\beta'=3$ we have $\mathbf{S}^{(1)}_{\beta\beta'}=S^{(1)}_{\beta\beta'}\mathbf{E}$, where E is a unit 3×3 matrix if $\beta=1$ or 2 and a 1×1 matrix at $\beta=3$. The functions $S^{(1)}_{\beta\beta'}$, $S^{(1)}_{44,\beta\beta'}$, and $S^{(2)}_{\beta\beta'}$ are connected by the relation

$$S_{\beta\beta'}(\mu,\mu')=\frac{\alpha_{\beta\beta'}}{\alpha_\beta/\mu+\alpha_{\beta'}/\mu'}H_\beta(\mu)H_{\beta'}(\mu') \tag{52}$$

with the functions $H^{(1)}_\beta$, $H^{(1)}_{r,\beta}$, and $H^{(2)}_\beta$, respectively.

The general solution of Eqs. (22) for $\mathbf{S}^R_{\beta\beta'}$ matrices is a linear combination of the functions $\cos m\psi$ and $\sin m\psi$ with $m=0$, 1, 2, while the matrix $\mathbf{S}^R_{\beta\beta'}(\Omega,\Omega')$ can be represented in the form of the expansion (12) by introducing the corresponding matrices $S^{(m)}_{R,\beta\beta'}(\Omega,\Omega')$. Substituting this expansion in (22) and integrating with respect to φ' we obtain three independent systems of equations that connect the matrices $S^{(m)}_{R,\beta\beta'}$ and $S^{(m)}_{\beta\beta'}$ with identical m. For the sake of brevity, we shall not write out these equations here. Thus, the problem of determining the $\mathbf{S}^R_{\beta\beta'}$ matrices can be reduced to integral equations of one variable. These equations can be solved exactly with a computer. They are also very convenient in a calculation by the iteration method, when account is taken of the finite number of the processes of polariton scattering in the volume and their reflection by the boundary.

The reflection and transmission coefficients $R_{\beta\beta'}$ and $T_{\beta\beta'}$ were calculated under the ABC (32). In this case the matrices $\mathbf{R}_{11}(\mu)$ and $\mathbf{T}_{11}(\mu)$ are determined by formulas (33)–(38), in which all three refractive indices n_β are real. In the calculation of the reflection coefficients $R_{\beta\beta'}(\mu)$ with $\beta\neq\beta'$ it must be recognized that

$$R_{\beta\beta',ij}(\mu)=\frac{n_\beta w_\beta}{n_{\beta'}w_{\beta'}}\frac{d\Omega_{\beta'}}{d\Omega_\beta}\frac{(E^{(\beta)}E^{(\beta)*})_i}{(E^{(\beta')}E^{(\beta')*})_j}. \tag{53}$$

Here $d\Omega_{\beta'}/d\Omega_\beta=(n_\beta/n_{\beta'})^2\mu_\beta/\mu_{\beta'}$; μ_β and $\mu_{\beta'}$ satisfy the relation $n_\beta^2(1-\mu_\beta^2)=n_{\beta'}^2(1-\mu_{\beta'}^2)$. The symbol $(E_l^{(\beta)}E^{(\beta)*})_i$ stands for one of the quantities $|E_l^{(\beta)}|^2$, $|E_r^{(\beta)}|^2$, $2\,\mathrm{Re}\,(E_l^{(\beta)}E_r^{(\beta)*})$, and $2\,\mathrm{Im}(E_l^{(\beta)}E_r^{(\beta)*})$, corresponding to the index $i=1$–4 at $\beta=1$ and 2, or for the quantity $|\mathbf{E}^{(3)}|^2$ at $\beta=3$, where $\mathbf{E}^{(\beta)}$ is the amplitude of the electric field of the wave β. The coefficients w_β relate the energy flux $\mathbf{J}_\beta$ of a plane monochromatic opto-exciton wave β with vector $\mathbf{E}^{(\beta)}$ (Ref. 18)

$$\mathbf{J}_\beta=\mathbf{n}_\beta w_\beta|\mathbf{E}^{(\beta)}|^2,\quad \mathbf{n}_\beta=n_\beta\Omega,$$

$$w_\beta=\frac{c}{8\pi}\left[1+\frac{M_0}{M}\left(\frac{n_\beta^2}{\varepsilon_0}-1\right)^2\right](\beta=1,2),\quad w_3=\frac{c}{8\pi}\frac{M_0}{M}. \tag{54}$$

In spectral reflection of one wave β from the boundary, there are excited in the general case waves of all three branches. We note that if $n_\beta>n_{\beta'}$ and $\mu_\beta<1-(n_{\beta'}/n_\beta)^2$, then the reflected wave β' attenuates in the interior of the crystal: $n_{\beta',z}=in_\beta[1-(n_{\beta'}/n_\beta)^2-\mu_\beta^2]^{1/2}$. When the inequalities (17) are satisfied, it suffices to take these damped waves into account only when the reflection coefficients are calculated, and their contribution to the energy transport can be disregarded.

The matrices $\mathbf{S}_{\beta\beta'}$ at $\omega>\omega_L$ were calculated in second order in $\tilde\omega_0$, i.e., scattering processes of order not higher than the second were taken into account. In the calculation of the matrices $\mathbf{S}^R_{\beta\beta'}$ we took into account only single reflections of the light, for which purpose it was sufficient to substitute in the integrand of (22) the approximate matrix $\mathbf{S}_{\beta\beta'}$ in place of $\mathbf{S}^R_{\beta\beta'}$. Thus, the results of the calculation at $\omega>\omega_L$, shown in the right-hand side of Figs. 4 and 5, are valid only if $\tilde\omega_0\ll1$.

On the short-wave edge of the spectrum, the quantity $T(1)/n^2$ for the wave 1 becomes very small, and the predominant contribution to the radiation is made by polaritons of the branch 2. In II–IV crystals, the inequality $M_0\ll M$ is satisfied. In this case the state densities of branches 2 differ greatly from those of 1 and 3: $g_2(\omega)\ll g_1(\omega)$, $g_3(\omega)$. Therefore on the short-wave section of the emission spectra, allowance for the scattering of the polaritons between the branches, compared with the case $M\to\infty$, leads to a decrease of the radiation intensity.

In the region of the longitudinal frequency ω_L, the predominant contribution to the radiation is made by polaritons of branch 1. The increase of $I(-0,\,1)$ with decreasing frequency is due to the increase of the coefficient $T(1)/n^2$ in the vicinity of the frequency ω_L. Thus, the $I(-0,\,1;\,\omega)$ emission spectrum has two maxima: a broad one near the frequency ω_0, and a narrower one at the frequency ω_L. It is of interest to note that the frequency dependence of the "branch 1–branch 1" Brillouin scattering efficiency, measured in Refs. 3 and 8, also has two maxima in the region of the longitudinal-transverse splitting. To illustrate the role of the longitudinal waves, Fig. 5 shows two sets of curves 1′–4′ and 1″–4″, calculated respectively with and without allowance for the states of the longitudinal waves in the kinetic equation for the polaritons.

We note in conclusion that the general method developed above for solving problems of transport theory in the presence of several branches of normal waves can be used also for problems connected with dragging of phonons, which likewise have longitudinal and transverse oscillation branches.

[1] We note that in contrast to Ref. 1 we do not separate the factor $\tilde\omega_0$. Therefore the S matrices in the present article correspond to the $\tilde\omega_0\mathbf{S}$ matrices of Ref. 1.

[2] For example, if unpolarized radiation is incident on the inner boundary, with an intensity independent of the propagation direction: $I(+0,\,\mu>0,\,\varphi)=\mathrm{const}$, then at $n\ll1$ or $n\ll1$ the effective transmission coefficient $\bar T$, which is equal to the ratio of the radiation-energy fluxes passing into the vacuum and incident on the boundary, is given by the expressions

$$\bar T=\frac{8}{n^3}\left(\frac{2}{3}-\frac{\ln n}{n}\right)\quad(n\gg1);\qquad \bar T=8n\left(\frac{2}{3}-n\ln\frac{1}{n}\right)\quad(n\ll1).$$

Thus, at $n\gg1$ or $n\ll1$ the effective reflection coefficient $\bar R=1-\bar T$ differs only insignificiantly from unity. At equilibrium, the ratio of the total fluxes incident on the inner and outer boundary of the crystals is equal to n^2 and the energy fluxes from the vacuum into the crystal and from the crystal into the vacuum coincide, so that $\bar T(1/n)=n^2\bar T(n)$.

[3] The contribution of the surface polaritons to the exciton luminescence in the opposite limiting case of strongly absorbing crystals is analyzed in Refs. 13 and 14.

[1]E. L. Ivchenko, G. E. Pikus, and N. Kh. Yuldashev, Zh. Eksp. Teor. Fiz. **79**, 1573 (1980) [Sov. Phys. JETP **52**, 793 (1980)].
[2]R. Ulbrich and C. Weisbuch, Phys. Rev. Lett. **38**, 865 (1977).
[3]G. Winterling and E. Koteles, Sol. State Commun. **23**, 95 (1977).
[4]P. Y. Yu and F. Evangelisti, *ibid.* **27**, 87 (1978).
[5]C. Hermann and P. Y. Yu, *ibid.* **28**, 313 (1978).
[6]W. C. Tait and R. L. Weiher, Phys. Rev. **178**, 1404 (1969).
[7]R. Zeyher, J. L. Birman, and W. Brenig, Phys. Rev. **B6**, 4617 (1972).
[8]P. Y. Yu and F. Evangelisti, Phys. Rev. Lett. **42**, 1642 (1979).
[9]V. M. Agranovich and M. D. Galanin, Perenos énergii élektrnnogo vozbuzhdeniya v kondensirovannykh sredakh (Energy Transport of Electronic Excitation in Condensed Media), Nauka, 1978, Chap. IV.
[10]S. Chandrasekhar, Radiative Transport, Oxford, 1950.
[11]V. M. Agranovich and V. L. Ginzburg, Kristalloptika s uchetom prostranstvennoĭ dispersii i teoriya éksitonov (Spatial Dispersion in Crystal Optics and the Theory of Excitons), Nauka, 1979, §11 [Wiley, 1967].
[12]V. M. Agranovich and T. A. Leskova, Pis'ma Zh. Eksp. Teor. Fiz. **29**, 151 (1979) [JETP Lett. **29**, 135 (1979)].
[13]V. M. Agranovich, S. A. Darmanyan, T. A. Leskova, and V. I. Rupasov, Izv. AN SSSR (ser. fiz) **43**, 1284 (1979).
[14]S. I. Pekar, Zh. Eksp. Teor. Fiz. **33**, 1022 (1957); **34**, 1176 (1958) [Sov. Phys. JETP **6**, 785 (1958); **7**, 813 (1958)].
[16]S. A. Permogorov, V. V. Travnikov and A. V. Sel'kin, Fiz. Tverd. Tela (Leningrad) **14**, 3642 (1972) [Sov. Phys. Solid State **14**, 3051 (1973)].
[17]S. A. Permogorov, A. V. Sel'kin, and V. V. Travnikov, *ibid.* **15**, 1822 (1973) [**15**, 1215 (1973)].
[18]A. Selkin, Phys. Stat. Sol. (b) **83**, 47 (1977).

Translated by J. G. Adashko